

Faraday Discussions

Accepted Manuscript



This manuscript will be presented and discussed at a forthcoming Faraday Discussion meeting. All delegates can contribute to the discussion which will be included in the final volume.

Register now to attend! Full details of all upcoming meetings: <http://rsc.li/fd-upcoming-meetings>



This is an *Accepted Manuscript*, which has been through the Royal Society of Chemistry peer review process and has been accepted for publication.

Accepted Manuscripts are published online shortly after acceptance, before technical editing, formatting and proof reading. Using this free service, authors can make their results available to the community, in citable form, before we publish the edited article. We will replace this *Accepted Manuscript* with the edited and formatted *Advance Article* as soon as it is available.

You can find more information about *Accepted Manuscripts* in the [Information for Authors](#).

Please note that technical editing may introduce minor changes to the text and/or graphics, which may alter content. The journal's standard [Terms & Conditions](#) and the [Ethical guidelines](#) still apply. In no event shall the Royal Society of Chemistry be held responsible for any errors or omissions in this *Accepted Manuscript* or any consequences arising from the use of any information it contains.

Title: A Surface Plasmon Enabled Liquid-Junction Photovoltaic Cell**Authors:** Woo-ram Lee¹, Syed Mubeen^{1,2}, Galen D. Stucky¹, Martin Moskovits^{1*}**Affiliations:**

¹Department of Chemistry and Biochemistry, University of California, Santa Barbara, CA 93106, USA.

²Department of Chemical and Biochemical Engineering, University of Iowa, Iowa 52242, USA.

*Correspondence to: moskovits@chem.ucsb.edu.

Abstract: Plasmonic nanosystems have recently been shown to be capable of functioning as photovoltaics and of carrying out redox photochemistry, purportedly using as charge carriers the energetic electrons and holes created following plasmonic decay. Although such devices currently have low efficiency, they already manifest a number of favorable characteristics, such as their tunability over the entire solar spectrum and a remarkable resistance to photocorrosion. Here we report a plasmonic photovoltaic using a 25 μm thick electrolytic liquid junction which supports the iodide-triiodide (I^-/I_3^-) redox couple. The device produces photocurrent densities in excess of $40 \mu\text{A cm}^{-2}$, an open circuit voltage (V_{oc}) of $\sim 0.24 \text{ V}$ and a fill factor of ~ 0.5 using AM 1.5 solar radiation at 100 mW cm^{-2} . The photocurrents and the power conversion efficiency were primarily limited by the low light absorption in the 2-D gold nanoparticle arrays. The use of a liquid junction greatly reduces dielectric breakdown in the oxide layers utilized, which for optimal performance must be very thin, leading to great improvement in the long-term stability of the cell's performance.

Main Text

Metallic nanostructures capable of supporting intense localized surface plasmon (LSP) resonances at visible frequencies, which have been known for many decades, are recently gaining significant attention for solar energy conversion applications.¹⁻¹⁷ Among the promising plasmon-enabled solar energy conversion strategies demonstrated are: (i) *light trapping* in which the optical properties of the plasmonic structured are exploited to improve the efficiencies of conventional semiconductor-based devices^{1,2} and (ii) producing devices which use the hot electrons and holes generated following LSP decay directly.^{3,4} Based upon the results reported to date, it is not unreasonable to hope that plasmonic systems will one day prove competitive with, and perhaps superior to traditional semiconductor-based devices as photovoltaics, or, more likely, as artificial photosynthesis devices, on account of the ease with which the light absorption properties of plasmonic systems can be tuned to encompass the entire intense portion of the solar spectrum, and the greater resistance of plasmonic systems to photo-corrosion, which has limited the use of semiconductors in artificial photosynthesis.⁵

Recent reports by us and others⁶⁻¹⁴ have convincingly demonstrated the fact that hot electrons and holes generated as a result of surface plasmon decay can be harvested to do useful work. One embodiment of such devices makes use of junctions between a plasmonic metal and an n-type semiconductor whose conduction band edge is more positive than the Fermi level of the metal. The Schottky barrier so formed creates the necessary internal potential barrier which hot electrons with sufficient energies can either overcome or tunnel through to become conduction electrons in the conduction band of the semiconductor. The electrons can then either be forced through a load generating electrical power, or transferred to an appropriate catalyst to carry out chemical reduction. The positive charges left behind can then act as holes completing

the circuit (in a photovoltaic device) or enabling chemical oxidation of an appropriate species through the intermediacy of an appropriate catalyst (in an artificial photosynthesis device).

While the plasmon-to-electron paradigm has been demonstrated in the context of photocatalysis, photosynthesis, and photodetection,^{5-7,11-14} its potential as a photovoltaic strategy has been less widely demonstrated.^{7,9-11,15-17} For example, we recently reported a solar cell device consisting of vertically oriented gold nanorods capped with a thin layer of TiO₂, in which all of the electrons and holes contributing to the solar-to-electric power generation were shown unequivocally to have had a plasmonic origin.⁷ Photoexcitation of the LSP resonance of the gold nanorods in that device ultimately resulted in the transfer of hot electrons to the conduction band of the TiO₂. A portion of the photon energy was converted to electron kinetic energy which appeared as open circuit photovoltage when collected by a low work function metal (titanium) electrode. A load connecting the two metals completed the circuit, maintaining electroneutrality and sustaining a measurable photocurrent. Despite its preliminary status, we were able to extract power with respectable absorbed photon-to-electron conversion efficiency of 2.75%.

However, based on the observed current-voltage characteristics and quantum efficiency measurements we concluded that high efficiency plasmonic solar cells could be realized if the quality of the semiconducting oxide layer can be substantially increased. In those devices, it was the thickness of the oxide layer that determined the cell efficiencies. As the oxide layer thickness was reduced, the cells' measured photovoltages decreased rapidly even if the photocurrents increased slightly. Such performance degradation, likely due to dielectric breakdown, is a common property of thin layers of most semiconducting oxides, attributed to current leakage caused by traps and defects generated either during the growth process or by electric stress created during the operation of the cell.^{18,19}

One way to minimize dielectric breakdown of thin oxides is by minimizing the damage at its interface. It is well established in electrolytic capacitors that the breakdown voltage of dielectric oxides can be substantially mitigated by using a liquid electrolyte.²⁰ The breakdown voltage follows a semi-log relationship with electrolyte resistivity and is independent of dielectric thickness.^{21,22} By choosing an electrolyte with modest conductivity, it is possible to increase the breakdown voltage and decrease the leakage currents. The electrolyte must also be electrochemically stable in the operational potential window and compatible with the electrode materials and the oxide.

We show here that the above approach can be successfully applied to developing plasmonic solar cells with stable photovoltages by fabricating a device based on Au nanoparticles coated with a thin layer of TiO₂, and investigating its photovoltaic behavior. Gold nanoparticles were chosen in lieu of gold nanorods to avoid ‘lightning rod’ effects at the metal/oxide interface.²³⁻²⁵ The TiO₂ was decoupled from the counter electrode using the iodide-triiodide (I⁻/I₃⁻) couple in a thin electrolyte layer.

The fabrication protocol and the corresponding cell configuration of the plasmonic metal/semiconductor/liquid junction solar cell are depicted schematically in Figure 1. Briefly, a 2 nm (mass thickness) gold film was e-beam deposited on a FTO-coated glass substrate. Rapid thermal annealing (RTA) of the gold coated FTO substrates at 400°C in a N₂ atmosphere converted the thin gold film into a 2-D array of gold nanoparticles with average diameters of ~17 nm and inter-particle distance of ~15 nm. A 5 nm layer of TiO₂ was subsequently deposited by atomic layer deposition (ALD) on the gold coated FTO substrate followed by thermal oxidation at 500 °C for 1 hour. Pt nanoparticles deposited on a second FTO coated glass served as the counter electrode. A 25 μm thick spacer constructed using electrically insulating thermal melt

polymer isolates the anode and the counter electrode and maintains the desired electrode-to-electrode spacing. The I^-/I_3^- electrolyte (0.1 M I_2 , 0.1 M lithium iodide (LiI), 0.6 M tetrabutylammonium iodide in acetonitrile) was injected between the two electrodes through pre-drilled holes, that were subsequently sealed. (See Methods for details).

Figure 2 shows the approximate energy positions of the plasmonic metal, semiconductor and the electrolyte. Au ($E_{F, Au} = 5.1$ eV vs. Vacuum) and TiO_2 ($E_{CB, TiO_2} = 4.2$ eV vs. Vacuum) form the plasmonic metal-semiconductor junction, creating a Schottky barrier of approximately 0.9 V at the metal–semiconductor interface.²⁶⁻²⁸ The I^-/I_3^- electrolyte was chosen, because of its proven performance in the field of dye sensitized solar cells. An important factor to consider is the location of the Fermi level (i.e. the electrochemical potential) of the I^-/I_3^- electrolyte with respect to the conduction band edge of the TiO_2 . Preferably, the acceptor level of the redox couple should be close to the conduction band edge of TiO_2 to extract conduction electrons efficiently. For the I^-/I_3^- electrolyte ($E_{F, I^-/I_3^-} = 4.8$ eV vs. Vacuum)²⁹ the redox potential is more positive (on the electrochemical scale) than the conduction band edge of TiO_2 , creating a barrier between TiO_2 and I^-/I_3^- . To circumvent this, we deposited 2 nm of titanium nitride (TiN) on top of the TiO_2 using ALD. The reported work function of ALD deposited TiN is 4.2-4.4 eV vs vacuum, which should make it a good material for forming an Ohmic contact with TiO_2 .³⁰ Additionally, since TiN is a good conductor, the interface between TiN and I^-/I_3^- would not sustain any electrical fields.

The photon-to-electron conversion in this device occurs as follows. Visible light is absorbed by the gold nanoparticles producing LSP excitations, which decay to a large number of hot electrons. Hot electrons with sufficient energies overcome the Schottky barrier at the metal-semiconductor junction and enter the conduction band of the TiO_2 . Some energetic hot carriers

might quantum mechanically tunnel through the barrier. The electrons conduct through the TiN layer to its surface where they carry out I_3^- to I^- reduction. The positive charges left in the gold conduct through the load where they carry out the oxidation step (I^- to I_3^-) on the Pt layer at the counter electrode, thereby restoring charge neutrality.

As in electrochemical dye-sensitized solar cells, this structure decouples the photon absorption process from charge separation and transport; however, it has the significant advantage that metals do not photobleach as dyes do.³¹ A key feature of this device is that the cell can be kept sufficiently thin to eliminate the uncompensated resistance losses due to the electrolyte that arise in typical electrochemical systems. The presence of electrolyte also increases the reliability of the cell by increasing the breakdown voltage and reducing leakage current.

Figure 3 displays the current density vs voltage characteristics of a representative device when illuminated by simulated AM1.5 solar radiation (100 mW cm^{-2}). The active area of the device was 0.80 cm^2 . Under AM1.5G conditions, we observed a short circuit current density of $46 \mu\text{A cm}^{-2}$, a stable open circuit voltage (V_{oc}) of 0.24 V, a fill factor of 0.48 and a power conversion efficiency of $\sim 0.005\%$. The short circuit current density and power conversion efficiency are limited by the low nanoparticle coverage and the consequently low photon absorption. Extinction measurements performed on a single 2D array of gold nanoparticle yield an extinction value of ~ 0.1 . (The absorbance would be less than this since some of the light extinction results from scattering.) Increasing the metal particle density or using cells in tandem would greatly improve the performance. Additionally, significant increases are expected by optimizing the reflection losses, electrode-electrolyte configuration and surface treatment, steps that are routinely used to improve the performance of conventional semiconductor devices.

Incorporating such improvements could increase the short circuit current and consequently the cell's efficiency by a factor of at least 20. Efforts to boost the open circuit voltage, such as those discussed below should produce further efficiency increases of at least a factor of 2.

In fact, a key result of this work is that despite using less than a monolayer of gold nanoparticles we were able to obtain short circuit current densities of $\sim 0.05 \text{ mA cm}^{-2}$, wholly powered by plasmon-mediated charge carriers. The modest fill factor is due to losses from concentration overpotentials and can be minimized by optimizing the electrode-electrolyte configuration. By reducing the inter-electrode distance between the anode and the cathode, other constraints such as absorption of light by the solution, insufficient conductivity of the electrolyte, uncompensated resistance losses can also be mitigated.

The semiconductor layer in our device does not take part in photon absorption, thus the semiconductor layer can be made very thin, essentially working uniquely as an electron filter. The maximum photovoltage depends on the Schottky barrier height between the metal and the semiconductor and on the redox potential of the electrolyte. Although what we report is a significant step in the achievable photovoltages for plasmonic solar cell system, the photovoltages obtained (0.24 V) are low. This is because the electrochemical potential of the selected redox couple was much more positive (on the electrochemical scale) than the conduction band of TiO_2 . By selecting a redox couple whose Fermi level is close to the conduction band of TiO_2 , one could significantly improve the photovoltages.

Conclusions:

We report a plasmonic photovoltaic using a $25 \text{ }\mu\text{m}$ thick electrolytic liquid junction which supports the iodide-triiodide (I^-/I_3^-) redox couple. The device produces photocurrent densities in

excess of $40 \mu\text{A cm}^{-2}$, an open circuit voltage (V_{oc}) of ~ 0.24 V and a fill factor of ~ 0.5 using AM 1.5 solar radiation at 100 mW cm^{-2} . The use of a thin liquid layer with redox active molecules between the electrodes results in a cell which does not deteriorate on account of dielectric breakdown in the thin oxide layers, providing the basis for the development of durable and efficient plasmonic photovoltaics using a wide choice of both amorphous and polycrystalline oxides and inexpensive redox active couples, which can yield high photovoltages without sacrifice in the overall power conversion efficiency that must often be made in solid-state cells, where material quality is more stringent. Indeed even these very preliminary cells meant to illustrate the principles showed remarkable longevity, their current and voltage characteristics remaining constant over multiple runs carried out over many weeks.

Methods:

The solar cell was fabricated on two FTO-coated glass substrates ($7 \Omega/\text{sq}$, 2.2 mm thickness, TCO22-7, Solaronix).

To prepare the cathode, the FTO glass was cleaned for 20 min. in a detergent solution (Deconex® 12 BASIC, Borer Chemie AG) using an ultrasonic bath, and rinsed with tap water, DI water and ethanol. A 2 nm (mass thickness) gold film was e-beam deposited on a FTO-coated glass substrate. Rapid thermal annealing (RTA) of the gold coated FTO substrates at 400°C in a N_2 atmosphere was carried out for 5 minutes to form a 2-D random arrangement of gold nanoparticles. TiO_2 and TiN layers were deposited in an Oxford FlexAl ALD tool. For TiO_2 , tetrakis(dimethylamino)titanium (TDMAT) and water were used as precursor and reactant, respectively, at 200°C , followed by thermal oxidation at 500°C in an oven for 1 hour. Plasma-enhanced ALD of TiN was carried out at 300°C using TDMAT and a mixture of H_2 and N_2 gas (3:1 ratio).

For the anode, two holes were drilled in the FTO glass, which had been washed as described previously. The FTO glass was coated with a thin layer of a 5 mM solution of $\text{H}_2\text{PtCl}_6 \cdot 6\text{H}_2\text{O}$ in isopropanol, dried at room temperature for 10 minutes, heated from room temperature to 450°C at a rate of $25^\circ\text{C}/\text{min}$ and maintained at 450°C for 20 minutes.

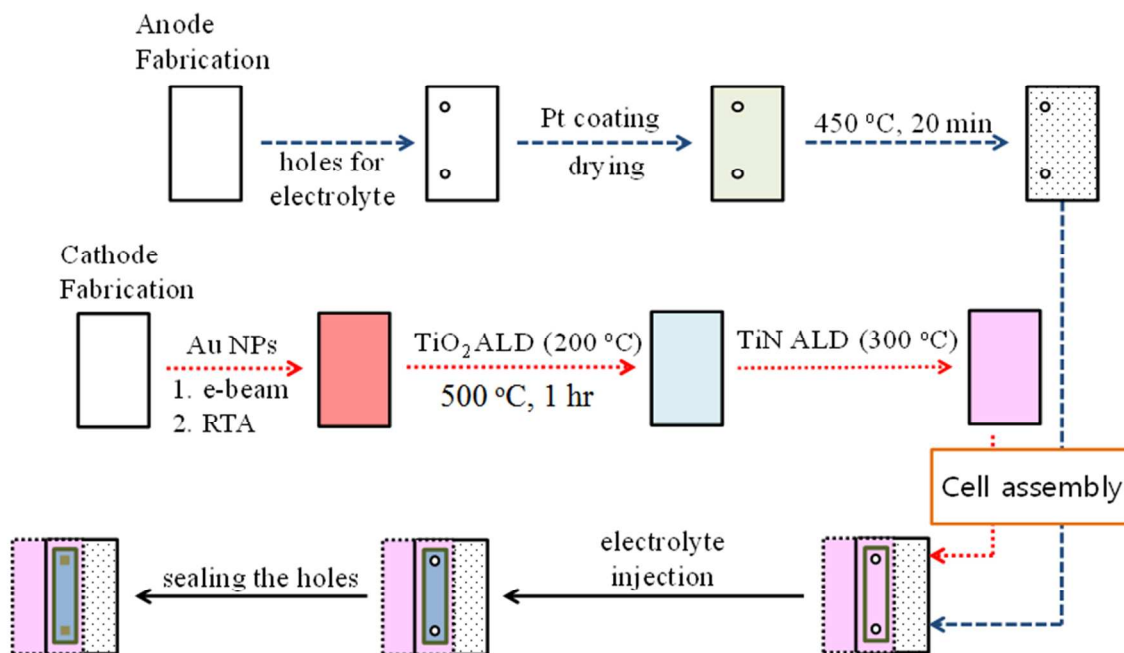
The two electrodes were sealed around their perimeter using a thermal melt polymer film (25 μm thickness, Meltonix 1170-25, Solaronix) such that a ~ 25 μm space was created between them. Liquid electrolyte (0.1 M I_2 , 0.1 M lithium iodide (LiI), 0.6 M tetrabutylammonium iodide in acetonitrile) was injected in the space between the electrodes through one of the holes pre-drilled in the anode, and the holes were sealed with thermal melt polymer films and microscope cover slips. The active area of the device was 0.80 cm^2 .

Photovoltaic measurements were carried out using a Newport Air Mass 1.5 Global (AM 1.5 G) full spectrum solar simulator as source at an irradiation intensity of 100 mW cm^{-2} . Current density-voltage (J - V) measurements were carried out using a Keithley 2400 Digital Source Measure Unit.

Acknowledgements: This work was supported by the Institute for Energy Efficiency, an Energy Frontier Research Center funded by the US Department of Energy, Office of Science, Office of Basic Energy Sciences (award no. DE-SC0001009). Two of us (GDS and WRL) wish to thank the National Science Foundation (DMR 0805148) for support. Support from the MRSEC Program of the National Science Foundation under Award No. DMR 1121053 is also gratefully acknowledged. We also made extensive use of the MRL Central Facilities at UCSB, a member of the NSF-funded Materials Research Facilities Network (www.mrfn.org).

Figures:

(a)



(b)

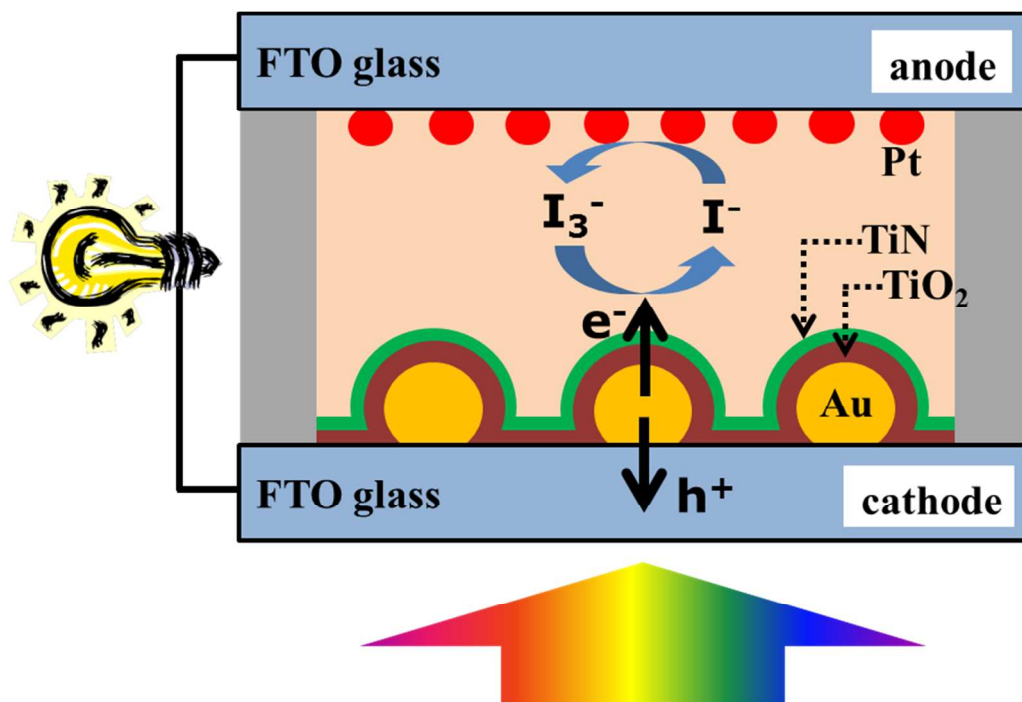


Figure 1. (a) Schematic itemizing the steps in the fabrication process used to produce the plasmonic liquid-junction photovoltaic cells. (b) A schematic of the structure, components and materials comprising the cell.

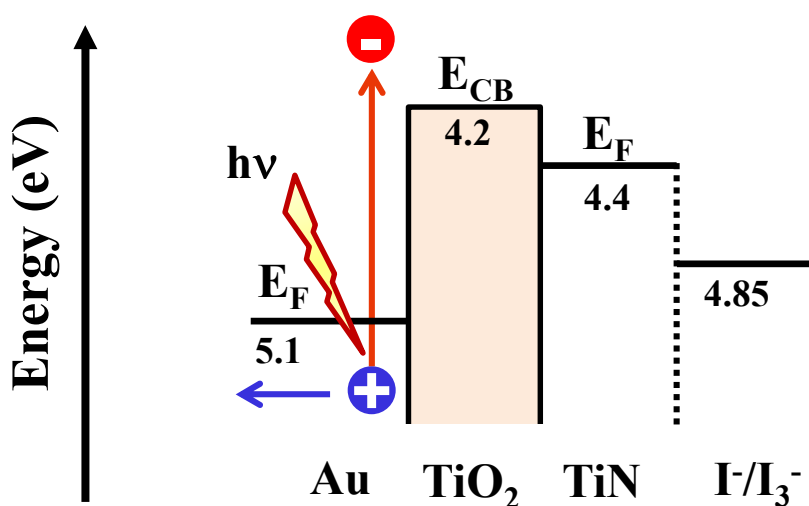


Figure 2. Energy band diagram depicting the electron transfer pathway. Hot electrons generated by surface plasmon decay enter the conduction band of TiO_2 by overcoming the Schottky barrier at the Au/TiO_2 interface. Charge carriers conduct through the Ohmic junction and into the TiN and ultimately to the I/I_3^- species in the electrolyte.

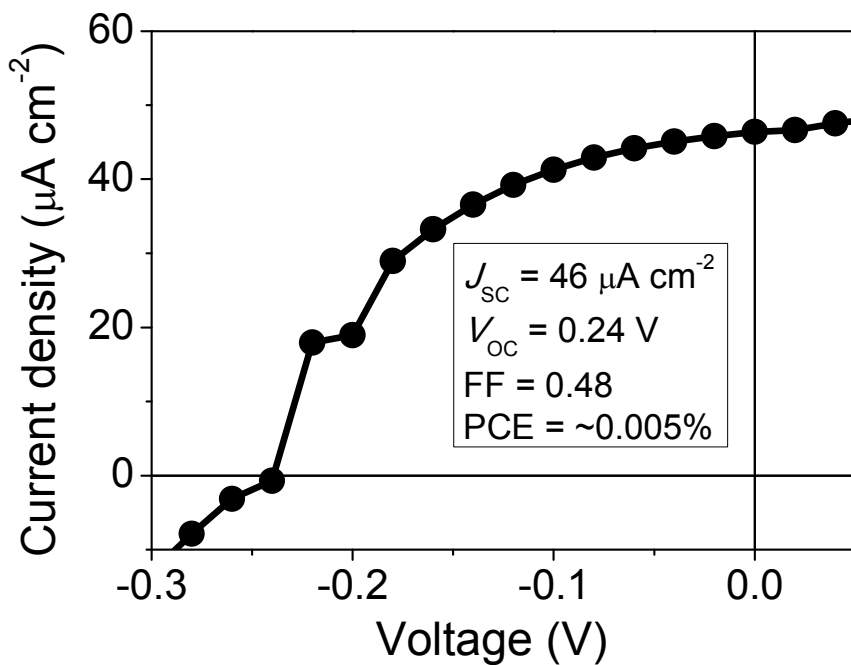


Figure 3: Photocurrent density vs voltage (J - V) measured under simulated AM1.5G full sun illumination (100 mW cm^{-2}) for a cell with an active area of 0.80 cm^2 .

References:

1. K. R. Catchpole, and A. Polman, *Opt. Express*, 2008, **16**, 21793.
2. H. A. Atwater, and A. Polman, *Nature Mater.*, 2010, **9**, 205.
3. C. Clavero, *Nature Photon.*, 2014, **8**, 95.
4. Manjavacas, J. G. Liu, V. Kulkarni, and P. Nordlander, *ACS Nano*, 2014, **8**, 7630.
5. S. Linic, P. Christopher, and D. B. Ingram, *Nature Mat.*, 2011, **10**, 911.
6. S. Mubeen, J. Lee, N. Singh, S. Krämer, G. D. Stucky, and M. Moskovits, *Nature Nanotech.*, 2013, **8**, 247.
7. S. Mubeen, J. Lee, W.-r. Lee, N. Singh, G. D. Stucky, and M. Moskovits, *ACS Nano*, 2014, **8**, 6066.
8. J. Lee, S. Mubeen,† X. Ji, G. D. Stucky, and M. Moskovits, *Nano Lett.*, 2012, **12**, 5014.
9. S. Mubeen, G. Hernandez-Sosa, D. Moses, J. Lee, and M. Moskovits, *Nano Lett.*, 2011, **11**, 5548..
10. F. Wang, and N. A. Melosh, *Nano Lett.*, 2011, **11**, 5426.
11. F. P. G. de Arquer, A. Mihi, D. Kufer, and G. Konstantatos, *ACS Nano* 2013, **7**, 3581.
12. Y. Nishijima, K. Ueno, Y. Kotake, K. Murakoshi, H. Inoue, and H. Misawa, *J. Phys. Chem. Lett.*, 2012, **3**, 1248.
13. M. W. Knight, Y. Wang, A. S. Urban, A. Sobhani, B. Y. Zheng, P. Nordlander, and N. J. Halas, *Nano Lett.*, 2013, **13**, 1687.
14. V. Subramanian, E. Wolf, and P. V. Kamat, *J. Phys. Chem. B*, 2011, **105**, 11439.
15. Y.-H. Su, Y.-F. Ke, S.-L. Cai, and Q.-Y. Yao, *Light: Sci. Appl.*, 2012, **1**, e14.
16. Z. H. Chen, Y. B. Tang, C. P. Liu, Y. H. Leung, G. D. Yuan, L. M. Chen, Y. Q. Wang,

- I. Bello, J. A. Zapien, W. J. Zhang, C. S. Lee, and S. T. Lee, *J. Phys. Chem. C*, 2009, **113**, 13433.
17. T. Bora, H. H. Kyaw, S. Sarkar, S. K. Pal, and J. Dutta, *Beilstein J. Nanotechnol.*, 2011, **2**, 681.
18. J.J. O'Dwyer, *The theory of electrical conduction and breakdown of solids*, Clarendon Press, Oxford, 1973.
19. M. Fröhlich, *Theory of dielectrics*, Oxford University Press, 1949.
20. M. Jayalakshmi, and K. Balasubramanian, *Int. J. Electrochem. Sci.*, 2008, **3**, 1196.
21. A. Guntherschulze, and H. Betz, *Elektrolytkondensatoren*, Technischer Verlag Herbert Cram, Berlin, 1952.
22. F. J. Burger, and J. C. Wu, *J. Electrochem. Soc.*, 1971, **118**, 2039.
23. P. F. Liao, and A. Wokaun, *J Chem. Phys.*, 1982, **76**, 751.
24. O. Benson, *Nature*, 2011, **480**, 193.
25. M. B. Mohamed, V. Volkov, S. Link, and M. A. El-Sayed, *Chem. Phys. Lett.*, 2000, **317**, 517.
26. E. W. McFarland, and J. Tang, *Nature* 2003, **421**, 616.
27. J. Y. Park, H. Lee, J. R. Renzas, Y. Zhang, and G. A. Somorjai, *Nano Lett.*, 2008, **8**, 2388.
28. J. Tang, M. White, G. D. Stucky, and E. W. McFarland, *Electrochem. Commun.*, 2003, **5**, 497.
29. J. Datta, A. Bhattacharya, and K. K. Kundu, *Bull. Chem. Soc. Jpn.*, 1988, **61**, 1735.
30. K. Choi, H.-C. Wen, H. Alshareefa, R. Harris, P. Lysaght, H. Luanc, P. Majhid, and B. H. Lee, Proceedings of Essderc 2005: 35th European Solid-State Device Research Conference, Book Series: Proceedings of the European Solid-State Device Research Conference, pp 101-104, 2005.

31. J. Kosar, *Light-sensitive systems*, Wiley, New York, 1965.